Microwave Frequency Divider With Tunable Division Factors Based on an Optoelectronic Oscillator

Liangzun Tang, Shifeng Liu, Li Yang, Zhenzhou Tang, Simin Li, and Shilong Pan, *Fellow, IEEE*

***Abstract*—A wideband microwave regenerative frequency divider with tunable division factors is proposed and experimentally demonstrated based on harmonic mixing in an optoelectronic oscillator. In the optoelectronic oscillation cavity, a phase modulator is cascaded with an optical filter to achieve equivalent intensity modulation by preserving the single sideband. Harmonic mixing procedure occurs between the $+1^{st}$-order sideband of the input signal and the higher-order sideband of the oscillation signal within the following photodetector. When the intermediate frequency generated by the harmonic mixing procedure matches the oscillation frequency, and the loop phase and gain conditions are satisfied, microwave regenerative frequency division can be achieved. The frequency division factor is determined by the order of the optical sideband of the oscillation signal during the harmonic mixing and can be adjusted using a two-tap microwave filter constructed with a phase shifter on each arm. Experimental results show that a microwave regenerative frequency divider with an operating frequency range of 22 to 30 GHz and division factors varying from 2 to 8 was successfully realized.**

***Index Terms*—Microwave photonics, optoelectronic oscillator, regenerative frequency divider.**

I. Introduction

MICROWAVE frequency divider plays an essential role in numerous applications, especially in modern radars [1], [2], wireless communication [3] and navigation systems [4]. By generating a phase-coherent subharmonic of the input signal, the frequency divider enables signal processing, phase noise optimization, frequency synthesis, and synchronization. Traditional electronic frequency dividers can be categorized into two main types: digital frequency dividers and analog frequency dividers. Digital frequency dividers offer flexible division factors but are limited to relatively low operating frequencies (several GHz). In contrast, analog frequency dividers can operate at significantly higher frequencies, but their division factors are generally fixed.

Recently, photonics-assisted microwave frequency dividers have attracted significant attention due to their notable benefits, such as broad bandwidth [5], excellent tenability [6], [7], and resistance to electromagnetic interference [8]. Most of these dividers are realized either through all-optical cavities or optoelectronic feedback systems. The frequency dividers utilizing all-optical cavities are typically implemented based on the nonlinear dynamical period-*N* state oscillation in an optically injected semiconductor laser [9] or Fabry-Perot laser [10]. Although a tunable division factor can be achieved using this approach, the operating frequency is discontinuous and limited by the modulation bandwidth of the lasers.

Frequency dividers that utilize optoelectronic feedback systems are typically implemented using either an optical phase-locked loop (OPLL) or an optoelectronic oscillator (OEO). For instance, in [11], a frequency divider is realized by employing an optical phase-locked loop to lock an optical frequency comb to the signal being divided. While this approach can achieve a very large frequency division factor and low phase noise, the system becomes complex and costly due to the cascading modulation and servo loop.

On the other hand, frequency dividers based on an OEO are generally implemented using either the injection-locking technique or the regeneration technique. Although the frequency dividers utilizing the injection-locking technique [12], [13] can achieve a tunable division factor, the output frequency is fixed and determined by the oscillating frequency of the free-running OEO. Frequency dividers that employ the regeneration technique operate by regenerating the signal from system noise through an optoelectronic oscillation loop [14], [15], [16]. However, earlier designs [14], [15] were limited to achieving only a single division factor. While one study [16] extended the division factor to a range of 2 to 6, it required adjusting the optical filter each time the division factor was changed to maintain proper amplitude and phase matching in the OEO.

In this letter, we propose a wideband microwave regenerative frequency divider (RFD) with tunable division factors based on harmonic mixing in an OEO. In the optical path of the OEO, a phase modulator (PM) and an optical band-pass filter (OBPF) are used in conjunction to achieve equivalent intensity modulation. The nonlinear modulation in the PM can generate high-order sidebands, allowing the RFD to attain a large division factor. In the electrical path of the OEO, a two-tap microwave filter with a phase shifter on each arm is employed to adjust the loop delay and gain. This configuration enables the precise achievement of the desired division factor

Received 20 February 2025; revised 8 June 2025; accepted 30 June 2025. Date of publication 3 July 2025; date of current version 9 July 2025. This work was supported in part by the National Key Research and Development Program of China under Grant 2022YFB2802704, in part by Jiangsu Funding Program for Excellent Postdoctoral Talent under Grant 2022ZB237, and in part by the National Natural Science Foundation of China under Grant 62271249 and Grant 62071226. *(Corresponding author: Shifeng Liu.)*

The authors are with the National Key Laboratory of Microwave Photonics, Nanjing University of Aeronautics and Astronautics, Nanjing 210016, China (e-mail: lztang@nuaa.edu.cn; sfliu_nuaa@nuaa.edu.cn; liyang_photonic@nuaa.edu.cn; tangzhzh@nuaa.edu.cn; lisimin@nuaa.edu.cn; pans@ieee.org).

Color versions of one or more figures in this letter are available at https://doi.org/10.1109/LPT.2025.3585525.

Digital Object Identifier 10.1109/LPT.2025.3585525

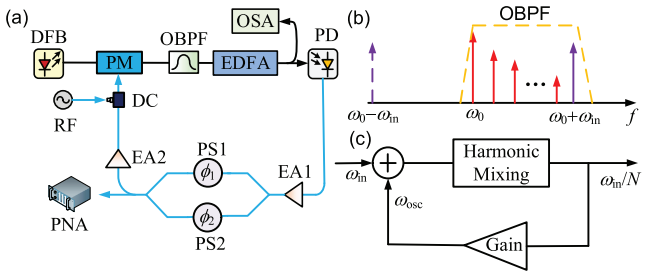

Fig. 1. (a) Schematic diagram of the proposed RFD based on an OEO. (b) Spectral diagram within the passband of the optical filter under the stable operation of the RFD. (c) Simplified schematic of the RFD operation. DFB: distributed feedback laser, PM: phase modulator, OBPF: optical band-pass filter, EDFA: erbium-doped fiber amplifier, OSA: optical spectrum analyzer, PD: photodetector, EA: electrical amplifier, PS: phase shifter, DC: directional coupler, RF: radio frequency, PNA: phase noise analyzer.

through appropriate gain and phase matching. Furthermore, the absence of a narrowband filter in the RFD facilitates a wide operating frequency range. Experimental results show that an RFD with an operating frequency range of 22 to 30 GHz and division factors varying from 2 to 8 is successfully realized.

II. Principle

The schematic diagram of the proposed RFD based on an OEO is depicted in Fig. 1(a). A continuous wave (CW) light emitted from a distributed feedback (DFB) laser is modulated by a PM, filtered by an OBPF, amplified by an erbium-doped fiber amplifier (EDFA), and then directed to a photodetector (PD). The PD converts the optical signal into an electrical signal, which is subsequently amplified and evenly distributed to the phase-shifter branches of the two-tap microwave filter. These signals are recombined via an electrical coupler and fed back to the phase modulator together with the injected signal. The two phase shifters are independently tunable, allowing for precise adjustment of loop delay and gain. Fig. 1(b) and (c) illustrate the spectral diagram within the passband of the optical filter under the stable operation of the RFD and the schematic of regenerative N-division based on a harmonic mixing effect, respectively. As can be seen, the $+1^{\text{st}}$-order sideband of the injected signal and the positive higher-order sidebands of the oscillating signal are all within the bandwidth of the OBPF.

Assume that the CW light can be represented as $E_0(t) = V_0\exp(j\omega_0 t)$. The injected signal and the oscillating signal of the OEO are expressed as $E_{\text{in}} = V_{\text{in}}\cos(\omega_{\text{in}}t + \theta_{\text{in}})$ and $E_{\text{osc}} = V_{\text{osc}}\cos(\omega_{\text{osc}}t + \theta_{\text{osc}})$, respectively. Here, V_0, V_{in}, V_{osc} denote the amplitudes, and ω_0, ω_{in}, ω_{osc} represent the angular frequencies. Therefore, the electric field of the optical signal output from the PM can be expressed as

$$E_{\text{PM}}(t) = V_0 \exp\left[j\omega_0 t + j\beta_{\text{in}}\cos(\omega_{\text{in}}t + \theta_{\text{in}}) + j\beta_{\text{osc}}\cos(\omega_{\text{osc}}t + \theta_{\text{osc}})\right] \tag{1}$$

where $\beta_{\text{in}} = \pi V_{\text{in}}/V_\pi$ and $\beta_{\text{osc}} = \pi V_{\text{osc}}/V_\pi$ are the modulation index of the injected signal and oscillating signal, respectively. Considering only the sidebands within the OBPF bandwidth and ignoring the small intermodulation harmonics, the optical signal output from the OBPF is given by

$$\begin{aligned} &E_{\text{OBPF}}(t) \\ &= J_0(\beta_{\text{in}})\left[J_0(\beta_{\text{osc}})E_0\exp(j\omega_0 t)\right. \\ &+ J_1(\beta_{\text{osc}})E_0\exp\left(j(\omega_0+\omega_{\text{osc}})t + j\left(\frac{\pi}{2}+\theta_{\text{osc}}\right)\right) \\ &+ J_2(\beta_{\text{osc}})E_0\exp\left(j(\omega_0+2\omega_{\text{osc}})t + j2\left(\frac{\pi}{2}+\theta_{\text{osc}}\right)\right) \\ &\left.+\ldots\right] + J_1(\beta_{\text{in}})J_0(\beta_{\text{osc}})E_0\exp \\ &\times\left(j(\omega_0+\omega_{\text{in}})t + j\left(\frac{\pi}{2}+\theta_{\text{in}}\right)\right) \end{aligned} \tag{2}$$

After amplifying by an EDFA, the optical signal undergoes photoelectric conversion in the PD. The photocurrent output from the PD can be expressed as

$$\begin{aligned} i_{\text{PD}} \propto\ &\Re A_0^2 J_0^2(\beta_{\text{in}}) \\ &\times\left[\sum_{i=0}^{n} J_i(\beta_{\text{osc}})J_{i+1}(\beta_{\text{osc}})\sin\left(\omega_{\text{osc}}(t-\tau)+\theta_{\text{osc}}\right)\right. \\ &+J_1(\beta_{\text{in}})J_n(\beta_{\text{osc}})\sin \\ &\left.\times\left((\omega_{\text{in}}-n\omega_{\text{osc}})(t-\tau)+\theta_{\text{in}}-n\left(\frac{\pi}{2}+\theta_{\text{osc}}\right)\right)\right] \end{aligned} \tag{3}$$

where $\Re$ represents the responsivity of the PD, n denotes the order of the sideband in the oscillating signal, and τ represents the time delay of the optical path. To achieve regenerative frequency division and maximum feedback gain, the output frequency components must have the same frequency and are phase-aligned. Additionally, the phase matching condition for feedback oscillation must be satisfied, thus

$$\begin{cases} \omega_{\text{osc}} = \omega_{\text{in}}/N \\ \theta_{\text{osc}} = \theta_{\text{in}}/N + (4k-N+1)\pi/2N \\ \omega_{\text{osc}}(\tau+h) = 2k\pi - \pi/2 \end{cases} \tag{4}$$

where $N = n+1$ represents the division factor, k is an integer corresponding to the order of the oscillation mode, and h denotes the total delay introduced by the electrical path. From Eq. (4), we can observe that an additional phase shift of $\pi/2$ is introduced to the oscillation signal through phase modulation. This additional phase shift enables different frequency division states to correspond to distinct phase matching conditions, particularly for even-order frequency divisions.

However, due to the non-flat frequency response of the OEO system within its operating range, it is difficult to precisely achieve different frequency division factors solely by adjusting the loop delay. To address this issue, a two-tap microwave filter is employed to precisely adjust the loop's amplitude and phase response, ensuring that different division factors align with optimal amplitude and phase matching conditions.

Assume that the microwave signal input to the two-tap microwave filter is $E_s\cos\omega t$, then the output microwave signal is given by

$$\begin{aligned} &E_{\text{out}}(\omega,t) \\ &= E_s\left[a(\omega)\cos(\omega t + h_1\omega) + b(\omega)\cos(\omega t + h_2\omega)\right]/2 \\ &= E_s E(\omega)\cos\left(\omega t + \phi(\omega)\right)/2 \end{aligned} \tag{5}$$

where

$$\begin{cases} E(\omega) = \sqrt{a^2(\omega)+b^2(\omega)+2a(\omega)b(\omega)\cos(h_2\omega - h_1\omega)} \\ \phi(\omega) = \arctan\left(\dfrac{a(\omega)\sin(h_1\omega)+b(\omega)\sin(h_2\omega)}{a(\omega)\cos(h_1\omega)+b(\omega)\cos(h_2\omega)}\right) \end{cases} \tag{6}$$

Here, $a(\omega)$, $b(\omega)$, h_1, and h_2 represent the amplitude response and delay response of the two arms, respectively. It can be seen that the amplitude and phase response of the two-tap microwave filter are related to both the oscillating frequency

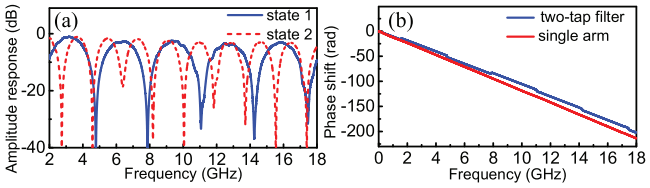

Fig. 2. (a) Magnitude response of the two-tap microwave filter in different states. (b) Phase response of the two-tap microwave filter and one of its arms.

and the delay in the two arms. When the phase difference between the upper and lower arms is kept constant, synchronous adjustment of the phase shifters enables independent tuning of the amplitude response. Conversely, varying the relative phase between the two arms allows for independent phase matching. Therefore, by adjusting the phase shifters, the gain and phase matching conditions required for an arbitrary division factor can be satisfied. Based on the theory of regenerative frequency division [17], the locking range of the RFD is given by

$$\Delta\omega_{\text{lock}} = \frac{\text{FSR}}{4\sqrt{\left(\sum_{i=0}^{n} J_i(\beta_{\text{osc}})J_{i+1}(\beta_{\text{osc}})/J_1(\beta_{\text{in}})J_n(\beta_{\text{osc}})\right)^2 - 1/2}} \tag{7}$$

where FSR is the mode spacing of the OEO. It can be observed that the locking range increases positively with the injected power.

III. Experiment Results

An experiment is carried out following the configuration depicted in Fig. 1(a). During the experiment, a CW light centered at 1550.24 nm with a power of 18.9 dBm is produced by a DFB laser. After passing through a PM (EOSPACE PM-DV5-40-PFA-PFA-LV), a tunable OBPF (Yenista XTM50), and an EDFA (Amonics AEDFA-PA-35-B-FA), the optical signal is injected into a PD (GD45220R-ku-1). The output electrical signal of the PD is amplified by an electric amplifier (EA1) with a gain of 20 dB and a bandwidth of 2-18 GHz, and then directed into a two-tap microwave filter. Each arm of the two-tap microwave filter incorporates a phase shifter with a bandwidth of DC-18 GHz. After passing through the microwave filter, the electrical signal is amplified by a second electric amplifier (EA2) with a gain of 27 dB and a bandwidth of 1-20 GHz and then fed back into the PM along with the injected signal output from an RF source (Agilent E8257D).

Prior to the experiment, the amplitude and phase response of the two-tap microwave filter were measured by a vector network analyzer (VNA, R&S ZNB40) as depicted in Fig. 2. As can be seen, the amplitude and phase response could be tuned by adjusting the phase shifters, corresponding to the tunable capability of gain and phase shift in different oscillation modes.

At the beginning of the experiment, the tunable OBPF was adjusted to position the optical carrier on the slope of its response, enabling the maximum operating bandwidth. The RF source was set to an output power of 15 dBm and a frequency of 22 GHz. By adjusting the phase shifters to set the OEO in a divide-by-2 state, the measured optical and electrical spectra of the OEO output are shown in Fig. 3. Fig. 3(a) illustrates

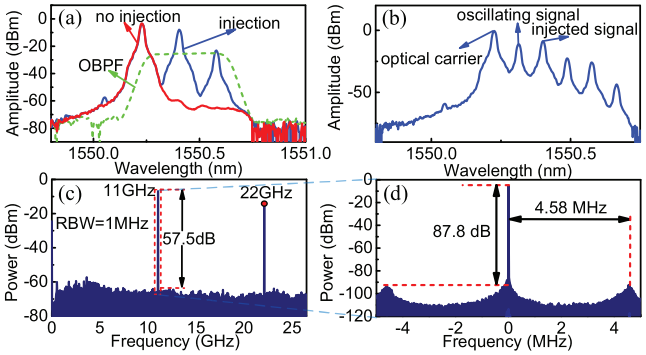

Fig. 3. Optical spectra of the OEO output (a) prior to oscillation and (b) in the divide-by-2 state. The electrical spectra of the 1/2 divided signal with a span of (c) 26 GHz and (d) 10 MHz.

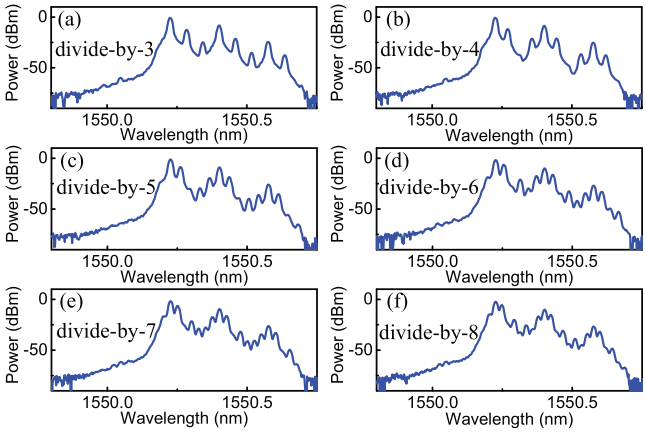

Fig. 4. Optical spectra of the OEO output with different division factors.

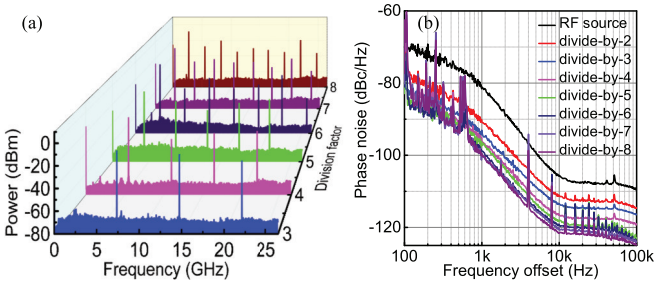

Fig. 5. (a) Electrical spectra of the OEO output with division factors ranging from 3 to 8. (b) Phase noise of the injected signal and the divided signals with division factors ranging from 2 to 8.

the magnitude response of the OBPF and the optical spectra of the OEO prior to oscillation. In Fig. 3(b), when the OEO is stably oscillating, a $+1^{\text{st}}$-order sideband of the oscillating signal appears between the optical carrier and the $+1^{\text{st}}$-order sideband of the injected signal. As shown in Fig. 3(c) and (d), the signal-to-noise ratio (SNR) of the 1/2 divided signal is approximately 57.5 dB at an RBW of 1 MHz. The RFD demonstrates a free spectral range (FSR) of about 4.58 MHz, with a side-mode suppression ratio exceeding 87.8 dB.

To demonstrate the tunability of the division factor, various division states were achieved by adjusting the phase shifters. Fig. 4 illustrates the optical spectra of the OEO output with division factors ranging from 3 to 8, while the corresponding

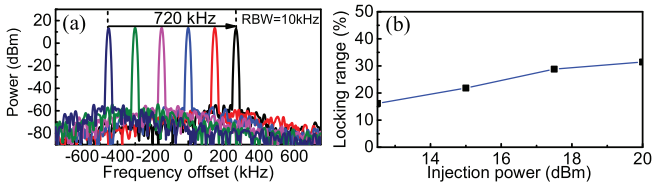

Fig. 6. (a) Locking range of the 1/2-divided signal with an injection power of 20 dBm. (b) The variation of locking ranging with different injected power in the divide-by-2 state.

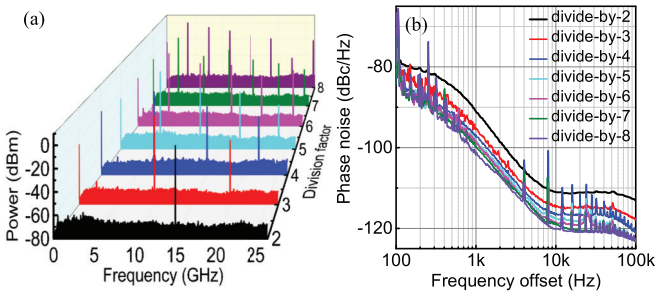

Fig. 7. (a) Electrical spectra of the OEO output and (b) phase noise of divided signals with division factors ranging from 2 to 8 under 30-GHz RF injection.

electrical spectra are presented in Fig. 5(a). It can be observed that the OEO generates multiple harmonics, which facilitate positive feedback through mixing with the injected signal. During practical implementation, suitable low-pass or band-pass filtering can be employed to effectively suppress the harmonic components.

To evaluate the phase noise performance of the divided signals, their phase noise was measured and compared with that of the injected signal, as shown in Fig. 5(b). For division factors ranging from 2 to 8, the phase noise of the divided signals improved sequentially by 5.6 dB, 7.5 dB, 11.0 dB, 12.5 dB, 13.8 dB, 15.1 dB, and 16.0 dB, respectively. According to the phase noise formula for regenerative frequency division, $S_{\mathrm{div}}(f) = S_{\mathrm{in}}(f)/N^2$, the experimental results align well with the theoretical values. Moreover, the phase noise curves show a significant spurious component around 4-kHz frequency offset, which is caused by imperfections in the second electric amplifier.

To investigate the stability of the RFD, the locking bandwidth of the OEO in the divide-by-2 state was measured with an injection power of 20 dBm, as shown in Fig. 6(a). The results indicate that the locking bandwidth of the 1/2 divided signal is approximately 720 kHz, which corresponds to a locking range of 31.44% for the injected signal. Fig. 6(b) illustrates the relationship between the locking range and the injection power. It can be observed that the locking range increases proportionally with the injection power.

To verify the operating bandwidth of the RFD, the frequency of the injected signal was set to 30 GHz. By adjusting the phase shifters, divided signals with division factors ranging from 2 to 8 were also successfully obtained. The corresponding electrical spectra of the OEO output and phase noise of divided signals are shown in Fig. 7. These results confirm that the RFD can effectively operate across a bandwidth of 22-30 GHz. In fact, depending on the device parameters, the system's operating bandwidth can theoretically range from 18 to 36 GHz.

IV. Conclusion

In conclusion, we propose and experimentally demonstrate a wideband RFD with tunable division factors based on harmonic mixing in an OEO. Two innovative key measures are adopted to enhance the system performance: one is the use of a PM combined with an OBPF to replace traditional intensity modulation, enabling higher-order nonlinear mixing effects and achieving a large division factor; the other is the use of a two-tap microwave filter to achieve precise tuning of the division factor. The experiment successfully demonstrates an RFD with tunable division factors ranging from 2 to 8 and an operating bandwidth of 22-30 GHz. The phase noise of the divided signals aligns well with the theoretical values. Furthermore, the RFD has a wide locking range, indicating its high stability.

References

[1] M. I. Skolnik, *Radar Handbook*, 3rd ed., New York, NY, USA: McGraw-Hill, 2008.
[2] S. Pan and Y. Zhang, "Microwave photonic radars," *J. Lightw. Technol.*, vol. 38, no. 19, pp. 5450–5484, Oct. 1, 2020.
[3] D. Tse and P. Viswanath, *Fundamentals of Wireless Communication.* Cambridge, U.K.: Cambridge Univ. Press, 2005.
[4] T. Hobiger, R. Haas, and J. S. Löfgren, "GLONASS-R: GNSS reflectometry with a frequency division multiple access-based satellite navigation system," *Radio Sci.*, vol. 49, no. 4, pp. 271–282, Apr. 2014.
[5] Y. Chen, P. Zuo, T. Shi, and Y. Chen, "Photonic-based reconfigurable microwave frequency divider using two cascaded dual-parallel Mach–Zehnder modulators," *Opt. Exp.*, vol. 28, no. 21, pp. 30797–30809, Oct. 2020.
[6] H. Chen and E. H. W. Chan, "Photonic microwave frequency divider with a tunable division ratio and harmonic suppression capability," *Opt. Exp.*, vol. 30, no. 19, pp. 34021–34033, Sep. 2022.
[7] H. Chen, M. Liu, A. Li, and E. H. W. Chan, "Microwave frequency dividers with reconfigurable fractional 2/N and 3/N division ratios," *IEEE Access*, vol. 11, pp. 29128–29137, 2023.
[8] H. Chen and E. H. W. Chan, "Ultra-simple all-optical microwave frequency divider," *IEEE Photon. Technol. Lett.*, vol. 34, no. 4, pp. 219–222, Feb. 4, 2022.
[9] S.-C. Chan and J.-M. Liu, "Microwave frequency division and multiplication using an optically injected semiconductor laser," *IEEE J. Quantum Electron.*, vol. 41, no. 9, pp. 1142–1147, Sep. 2005.
[10] M. Zhang, T. Liu, A. Wang, J. Zhang, and Y. Wang, "All-optical clock frequency divider using Fabry–Perot laser diode based on the dynamical period-one oscillation," *Opt. Commun.*, vol. 284, no. 5, pp. 1289–1294, Mar. 2011.
[11] D. Han, W. Wei, Z. Liu, W. Xie, and Y. Dong, "Sub-terahertz photonic frequency divider with a large division ratio based on phase locking," *Opt. Lett.*, vol. 46, no. 17, pp. 4268–4271, Sep. 2021.
[12] Y. Xu et al., "Injection-locked millimeter wave frequency divider utilizing optoelectronic oscillator based optical frequency comb," *IEEE Photon. J.*, vol. 11, no. 3, pp. 1–8, Jun. 2019.
[13] Y. Meng, T. Hao, W. Li, N. Zhu, and M. Li, "Microwave photonic injection locking frequency divider based on a tunable optoelectronic oscillator," *Opt. Exp.*, vol. 29, no. 2, pp. 684–691, Jan. 2021.
[14] S. Liu, K. Lv, J. Fu, L. Wu, W. Pan, and S. Pan, "Wideband microwave frequency division based on an optoelectronic oscillator," *IEEE Photon. Technol. Lett.*, vol. 31, no. 5, pp. 389–392, Mar. 5, 2019.
[15] H. Zhou et al., "Broadband two-thirds photonic microwave frequency divider," *Electron. Lett.*, vol. 55, no. 21, pp. 1141–1143, Oct. 2019.
[16] S. Duan et al., "Photonic-assisted regenerative microwave frequency divider with a tunable division factor," *J. Lightw. Technol.*, vol. 38, no. 19, pp. 5509–5516, Oct. 12, 2020.
[17] A. Safarian, S. Anand, and P. Heydari, "On the dynamics of regenerative frequency dividers," *IEEE Trans. Circuits Syst. II: Exp. Briefs*, vol. 53, no. 12, pp. 1413–1417, Dec. 2006.